Quantitative Structure-Activity Relationship Analysis of the Cation Permeability of the P2X2 Channel

Peter P. Mager*, Anje Weber and Peter Illes

Institute of Pharmacology and Toxicology, University of Leipzig, Saxony, Germany

Abstract: The membrane-embedded, ligand-gated P2X glycoprotein receptor is a monovalent-bivalent cation channel that is activated by physiological concentrations of extracellular ATP. A quantitative structure-activity relationship (QSAR) analysis was developed to model the cation permeability of the P2X2 channel and its mutants. As chemical properties, the helix-coil equilibrium constants and the distribution coefficients of the system octanol/water at pH 7.4 were applied and modified (sliding windows) according to Eroshkin *et al*. (*Comput. Appl. Biosci*., **1995**, *11*, 49-44). The results were visualized by a dimeric P2X2 channel construct. The results support the hypothesis that residues which put into the cavity and contribute to hydrogen bonding forces are involved to a control of the transport of hydrated cations through the P2X2 channel. The model may be useful to develop P2X2 receptor antagonists.

Key Words: Molecular modelling, structural bioinformatics, quantitative structure-activity relationship, QSAR, nonleast-squares regression analysis, P2X receptor, P2X2 receptor subunit, cation channel, calcium permeability, helix-coil equilibrium constant, distribution coefficient.

INTRODUCTION

The membrane-embedded, ligand-gated P2X receptor is a monovalent-bivalent cation channel-forming protein that is activated by physiological concentrations of extracellular adenosine 5'-triphosphate (ATP). The P2X receptor plays a role in the fast synaptic transmission between neurons and from autonomic nerves to smooth muscles. Currently, seven different P2X receptor proteins (P2X1 to P2X7) have been cloned. The P2X proteins have been divided into five subsequences (fragments): two intracellular cytoplasmic domains (N-terminal ICD1 and C-terminal ICD2), two transmembrane domains (N-terminal TMD1 and C-terminal TMD2), and a N-glycosylated extracellular sulfur-rich loop (ECD) with ATP binding sites. For reviews, see refs. [1,2]. There are differences between the "orthodox ion channels" and the membrane-embedded P2X ion channels. In this paper, it is hypothesized by a QSAR model that amino acid residues which put into the cavity and contribute to hydrogen bonding forces are involved in the control of the transport of hydrated cations through the P2X2 channel. A replacement of these residues by nonpolar hydrophobic amino acids may destroy the binding with hydrated cations and, in addition, may sterically hinder the cationic flux. The results are visualized using a dimeric P2X2 channel construct.

MATERIAL AND METHODS

The primary SWISS-PROT accession number of the rat P2X2 receptor subunit is P49653 (*rattus norvegicus*). In medicinal chemistry, the technique of alignment analysis [3] used here belongs to the basic knowledge. Alignment analysis was carried out in three steps: all sequences were compared to each other (pairwise alignments), a dendogram was constructed describing an approximate grouping of sequences by similarity, and the final alignment was carried out using the dendogram as guide. The PAM100 Dayhoff protein weight matrix was applied to weight different pairs of aligned amino acids. The following pairwise alignment parameters were used: gap penalty = 3, size of matching fragments (K-tuple) = 1, number of K-tuple matches on each diagonal in the dot matrix (top diagonals) = 5, number of diagonals around each of the best diagonals (window size) = 5. The following multiple alignment parameters were used: penalty for opening up a gap (fixed gap penalty) = 5, floating gap penalty = 10.

As biological parameter, the P2X2 permeability of Ca^{2+} in relation to Cs^{+} [4] was used. As chemical properties, the helix-coil equilibrium constants [5] and the distribution coefficients of the system octanol/water at pH 7.4 (taken from [6], calculated by using the Pallas software, CompuDrug Chemistry Ltd., Budapest, Hungary) were applied (Table **1**).

Regions of a protein that traverses a membrane consist often of apolar α-helices. It is believed that the Kyte-Doolittle approach [7] is only suitable for detecting transmembrane proteins with a high α-helix content. However, a lipophilic environment of proteins increases the probability to form a stable secondary structure, independently of its conformational type. This conclusion is supported by the fact that the old belief that the helix-coil equilibrium constant is primarily driven by the hydrophobicity at physiological pH values is wrong. The hydropathy index of Kyte-Doolittle correlates only with the lipophilicity or the apolar substituent constant (octanol/water) but not with the index of

*Address correspondence to this author at the Research Group of Pharmacochemistry, Institute of Pharmacology and Toxicology, University of Leipzig, D-04107 Leipzig, Härtelstr. 16-18, Saxony, Germany; Tel: +49(0)0341972463-2; Fax: -9; E-mail: magp@medizin.uni-leipzig.de

1573-4064/05 $50.00+.00

Table 1. Scores of the Physicochemical Parameters [5,6]. The Order of Values Correspond to the Order ACDEFGHIKLMNPQRSTVWY of the Amino Acids.

Helix-coil equilibrium constant:							
1.08	0.95	0.85	1.15	1.10	0.55	1.00	1.05
1.15	1.25	1.15	0.85	0.71	0.95	1.05	0.75
0.75	0.95	1.10	1.10				
Logarithm of the distribution coefficient P at pH 7.4:							
-2.74	-2.51	-5.60	-5.14	-1.54	-3.08	-1.91	-1.88
-4.79	-1.70	-2.28	-3.47	-2.83	-3.62	-5.50	-4.15
-3.26	-2.39	-0.56	-1.92				

the frequency of helices. Using the data of Table **1**, it can be seen that the correlation coefficient between the two variables is $r = 0.22$, it is clearly insignificant at the 5% level.

The structures of the studied peptide subsequences of the P2X2 channel are listed in Table **2**. The residues that contribute to the channel do not have sharp boundaries of their structural properties. Therefore, a sort of smoothing is necessary. The used minimum frame (min) is equivalent

Table 2. Subsequences of the Wild-type (WT01) and of the Site-directed Mutagenesis (MUT02 to MUT15) of the Rat P2X2 Receptor Subunit (Amino Acid Positions 330-349 of the Wild-type). As Biological Activity Parameter of the Native P2X2 Protein and P2X2 Mutants, the Experimentally Obtained Permeability of Ca^{2+} in Relation to that of Cs^{+} [4] was used (*Y*). The α-helix Periodicity Moments (fac-1) of the Sites 1-20 and the Averages (fac-2) of the Sites 4-11 were Determined from the Logarithm of the Distribution Coefficient P (Octanol/Water) at pH 7.4 and the Helix-coil Equilibrium Constant (Table 1). The Last Amino Acid (W) of the Intracellular Part of the Channel is Not Listed in the Table.

Fragments with sites		**Biological parameter *Y***	**Chemical terms**	
Compound	**1 10 20**		**fac-1**	**fac-2**
WT01	TIINLATALTSIGVGSFLCD	2.74	0.216	0.970
MUT02	TIINLATALTSIGVGSFLCE	2.96	0.207	0.970
MUT03	TIINLATALTSIGVGSFLCN	2.42	0.192	0.970
MUT04	TIIQLATALTSIGVGSFLCD	2.76	0.216	0.983
MUT05	TIIYLATALTSIGVGSFLCD	2.02	0.239	1.001
MUT06	TIIILATALTSIGVGSFLCD	1.21	0.240	0.995
MUT07	VIINLATALTSIGVGSFLCD	2.72	0.184	0.995
MUT08	YIINLATALTSIGVGSFLCD	3.79	0.168	0.970
MUT09	TIINLAVALTSIGVGSFLCD	1.57	0.257	0.995
MUT10	TIINLATALVSIGVGSFLCD	1.61	0.252	0.995
MUT11	TIINLATALYSIGVGSFLCD	0.33	0.273	1.014
MUT12	TIINLATALTAIGVGSFLCD	1.49	0.257	1.011
MUT13	TIINLATALTYIGVGSFLCD	0.08	0.286	1.014
MUT14	TIINLATALTSIGVGAFLCD	3.00	0.154	0.970
MUT15	TIINLATALTSIGVGYFLCD	3.33	0.121	0.970

with the window width in the analysis of the Kyte-Doolittle approach applied to predict transmembrane domains [7]. The maximum frame (max) is identical with the number (N) of sites (Table **2**).

A key factor was to avoid a "hydrophobic mismatch" (significant difference between the thickness of the membrane and the length of the transmembrane segments of the channel construct). A sliding window of 17-21 is equivalent to about 40 Angstroms, that is, the average thickness of a membrane. The moments of the α-helix periodicity (number of residues per cycle) moments were calculated according to Eisenberg [8]. The α-helix periodicity moment related to the lipophilicity (moving frame: min = 17, max = 20) was termed factor-1 (fac-1). It was assumed that $n \geq 4$ amino acids are needed in a string of n+2 residues to give clear tendency to form a helical domain. Therefore, the averages related to the helix-coil equilibrium constant are determined by using a sliding window of 4. The average related to the helix-coil equilibrium constant (moving frame: min = 4, max = 20) was termed fac-2. The parameters fac-1 and fac-2 were calculated by employing an algorithm proposed by Eroshkin *et al*. [9].

The parameters were correlated against the P2X2 permeability. Two approaches were applied, (i) regression analysis methods and, for comparisons, (ii) artificial neural network (ANN) techniques. The algorithms of the ordinary least-squares, principal-component, nonleast-squares (NLS) regression, and diagnostic statistics were presented in a monograph [10]. In addition, partial-least squares regression was applied [11,12]. Two ANNs were performed, a generalized regression (GRNN) genetic artificial neural network and an optimized backpropagation neural network, using the default parameters given elsewhere [13,14].

To visualize the prediction results at an atomistic level, the dimeric channel construct of the rat P2X3 receptor [2] was used as template protein for a P2X2 channel model. The amino acids of the pore-forming motif of the wild-type rat P2X2 receptor subunit are given in Table **2** (WT01). The extracellularly occuring third nucleoside binding domain (NBD3) that is probably involved in the gating mechanism of P2X receptors includes NFRFAKYY in P2X3 (279-286), it is in close steric neighborhood of the transmembrane part of the door of the pore-forming motif. The model of an open P2X channel presupposes that ATP is complexed with the NBD3. The geometry optimized ATP was placed in the binding site of the pseudoreceptor RFAKY. Then, the changes of the permeability of the mutant P2X2 protein predicted by the QSAR analysis were structurally visualized by the HyperChem molecular modelling program (Hypercube Inc., 419 Phillip Street, Waterloo, Ontario N2L 3X2, Canada).

RESULTS AND DISCUSSION

Quantitative Structure-Activity Relationship Analysis

Regarding Table **1** of the experimental paper [4], we see that a permeability index of the mutants D349E and D349N is 2.96 ± 0.22 and 2.42 ± 0.21. Inasfar, the variability is tolerable. It may be believed that these mutants not elicit a remarkable response compared with the wild-type P2X2, so the predictions of the permeabilities of these mutants are not relevant. This is wrong because this site represents one of the most important channel functions, and its inclusion is necessary to get a symmetric distribution of activity levels.

The chemical factors (fac-1, fac-2) were estimated from Table **1** according to the procedure described in the previous section. The results of the multiple alignment analysis, the permeability (Y), and the chemical factors are listed in Table **2**. Ordinary-least squares (OLS) regression which was introduced by Hansch and Fujita in QSAR analysis (review see [17], for example) leads to:

$$Y = 37.56 - 8.96(\text{fac-1}) - 33.93(\text{fac-2}) \quad (1)$$

The squared multiple correlation coefficient $R^2 = 0.86$ is significantly different from zero at the 5% level or less (the largest-root criterion 0.393 is here applied for hypothesis testing, it includes the commonly used F-test as special case). The test statistics for examining the regression coefficients are $TS1 = 1.77$ (fac-1) and $TS2 = 2.55$ (fac-2). Although the simple linear correlation coefficient $r1 = -0.880$ is significant (Table **3**), the corresponding regression coefficient $b1 = 8.96$ is insignificant ($TS1 = 1.77 < c1 = 2.54$ where $c1$ is the critical quantile of the Bonferroni criterion). This is the first evidence for an inconsistency.

To test this assumption, the intercorrelation coefficient r(fac-1,fac-2) = 0.867 must be considered (Table **3**. Since there are only two regressors (fac-1, fac-2), the estimated internal determination coefficient $D = 0.751$ is identical with the squared correlation coefficient $r^2 = (0.867)^2$ between the regressors. Its significance shows clearly that there is a collinear regressor set (a multicollinearity includes the collinearity as special case). Therefore, hypothesis testing of the OLS regression coefficients must be considered with caution because collinear ($c = 2$ regressors) and multicollinear regressor sets ($c \geq 2$) give misleading (i) estimates of the OLS regression coefficients, (ii) test statistics for examining these regression coefficients (such as

Table 3. Matrix of the Correlation Coefficients of the Data of Table 2. Significant Values are Indicated by an Asterisk (Studentized Maximum Modules Test [10], Significance Level α = 0.05, Critical Quantile = 0.642).

Variables	*Y*	fac-1	fac-2
Y	1.000	-0.880*	-0.903*
fac-1	-0.880*	1.000	0.867*
fac-2	-0.903*	0.867*	1.000

*TS*1, see above), and, in consequence, (iii) predictions, independently of the degree of the goodness-of-fit criterion [10].

In QSAR literatur it is often stated that it is standard practice to look at the collinearities to conclude whether a Hansch-Fujita QSAR analysis would be appropriate. There are many cases that this conclusion is incorrect. For example, consider a simple (4,4)- intercorrelation matrix with correlation coefficients of -1/3 between the descriptors (sample size = 20). Although -0.33 is insignificant, the least eigenvalues of the correlation matrix of the descriptors is exactly zero. This implies that the correlation matrix (or the corresponding dispersion matrix) cannot be inverted, and the solution of a regression system collapses numerically due to a "perfectly created" multicollinearity (the descriptor matrix is completely ill-conditioned). Therefore, the inspection of an intercorrelation matrix alone is wholly incapable of diagnosing QSAR data [19], and more sophisticated methods are needed.

Diagnostic statistics [10] led to the result that the design matrix (Table **2**) does not have significant (i) high-leverage points (diagonal elements of the hat matrix), (ii) influential points (likelihood function distance criterion), and (iii) outliers (externally Studentized residuals). Because of (i), the MC is not based on high-leverage points of the regressor matrix.

To tackle the problem of collinearity and multicollinearity, various alternatives have been developed, such as (i) ridge regression, (ii) latent-root regression, (iii) Hotelling's regression upon principal components (principal-component regression analysis, PCRA), (iv) nonleast-squares (NLS) regression [10], and (v) partial-least squares (PLS) regression [11,12].

It is often assumed by medicinal chemists that a QSAR model can only be properly asssessed by bootstrapping resampling (a linear approximation of bootstrapping is the one-leaving-out jackknifing). From the bootstrap samples, estimators and test statistics can be assessed but it is well known that the present-day resampling theories for constructing point and interval statistics require further development. Only if the total sample size tends to infinity and under a homoscedastic error model, the estimators are asymptotically unbiased and consistent. Resampling may only be useful for diagnostic statistics, however [18].

Using PCRA to test the type of the collinearity, two principal components (PC1, PC2) that were derived from the two regressors (fac-1, fac-2). The PC1 and PC2 were regressed against the activity parameter:

$$Y = 2.14 - 0.99(PC1) + 0.05\ (PC2) \qquad (2)$$

The squared multiple correlation coefficient is equal to that estimated in eq. (1). The test statistics are $TS1 = 8.35$ and $TS2 = 0.40$ (critical quantiles as above). There is an isotonic rank order of the regression coefficients which are completely unaffected by an omission. The absolute scores of the regression coefficients and the test statistics decrease monotonically, that is, there is a hierarchy of the meaning of the components. The percentage of the information content can be determined by the eigenvalues ($\lambda 1$, $\lambda 2$) of the correlation matrix of the chemical descriptors. The percentages are 93.33% and 6.67%. As $\lambda 2$ (test on zero eigenvalues of the intercorrelation matrix according to Bartlett) and PC2 are insignificant (TS2 = 0.40), PC2 must be omitted. The test statistics for examining the remaining regression coefficient is $TS1 = 8.63$ (the critical quantile of the Bonferroni criterion is equal to 2.16 at the 5% significance level). The apparent drawback of a small loss of information (6.67%) is overcompensated by a higher predictive model power, i.e., the capacity to represent correctly those data that were not members of the training set. It is often suggested that the standard error (s = 0.43) associated with the regression equation is useful. However, its use does not give deeper insight because its value depends on the scaling of the regressand. The null hypothesis of a zero standard error cannot be examined because no test is available. Retransformation of eq. (2) leads to the NLS regression equation:

$$Y = 32.862 - 10.943(fac\text{-}1) - 28.734\ (fac\text{-}2) \qquad (3)$$

which should be compared with the OLS regression model given in eq. (1). The squared multiple correlation coefficient $R^2 = 0.85$ is significantly different from zero at the 5% level or less (the largest-root criterion is 0.264), it differs not significantly from that of eq. (1). Although diagrams prove nothing, they bring outstanding features readily to the eye. This visual survey provides the experimenter that the model is likely appropriate. Fig. (**1**) illustrates the plot of the experimentally measured against the theoretically calculated values using eq. (3).

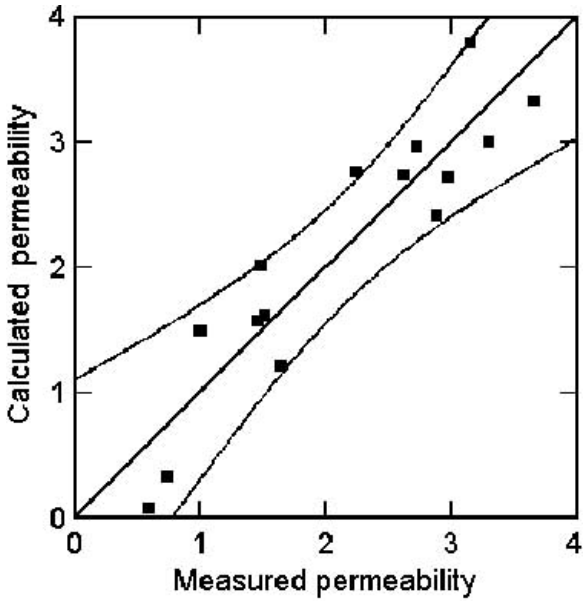

Fig. (1). Experimentally obtained permeability of Ca^{2+} in relation to that of Cs^+ (P2X2 and mutants of P2X2 [4]), and theoretically calculated permeability by inserting the scores of fac-1 and fac-2 (Table 2) into a QSAR equation estimated by NLS regression [eq. (3)]. The 95% confidence interval is shown.

Sometimes it is believed that the degree of collinearity will inflate the error estimates of the regression coefficients of a regression equation. This statement is incorrect with

respect to eqs. (2) and (3) but correct for eq. (1). Eq. (2) represents the PCRA equation, that is, the two components are orthogonal. Eq. (3) includes the reduced-rank model with the statistically significant component PC1. It was retransformed in terms of the original regressors according to the algorithm described in [10] in order to interpret physically the result. Eqs. (3) includes the biased but efficient and consistent estimators for which the influence of collinearity was removed.

PLS regression [11,12] led to a similar result. The squared multiple correlation coefficient is $R^2 = 0.85$, and the unscaled PLS regression equation is equal to:

$$Y = 33.203 - 10.804(\text{fac-1}) - 29.110(\text{fac-2}) \quad (4)$$

Hypothesis testing by simultaneous statistical inference theory is not included into the PLS regression algorithm, however.

Only for comparison, the weight coefficients of an optimized backpropagation (BP) neural network are collected in Table **4**. The squared multiple correlation coefficient R^2 = 0.90 is highly significant (critical quantile see above), the standard deviation is 0.33 (maximum error = 0.71). Fig. (**2**) illustrates the plot between the experimentally obtained and theoretically calculated scores of a permeability. There is a single outlier beyond the 95% confidence limits (compound 6, i.e., MUT05). The best squared multiple correlation coefficient (R^2 = 0.997) was obtained by a generalized regression genetic neural network (GRNN) which employed two inputs, two hidden layers (default), and one output neuron (direct transfer function). Selection of the chemical variables fac-1 and fac-2 (inputs) was performed by the top 50% surviving, refilling of the population by cloning the survivors, mating by the TailSwap technique, and mutation exchange technique at a rate of 25%. As expected, the two inputs were categorized as useful, and the genetic algorithm did not omit a variable. However, the models are probably somewhat (BP) or strongly overfitted (GRNN) and not further considered, therefore.

Taken the results together, the hypothesis is supported that the α-helix periodicity moment related to the lipophilicity and the average related to the helix-coil equilibrium constant determine the the P2X2 permeability of Ca^{2+} in relation to Cs^{+}.

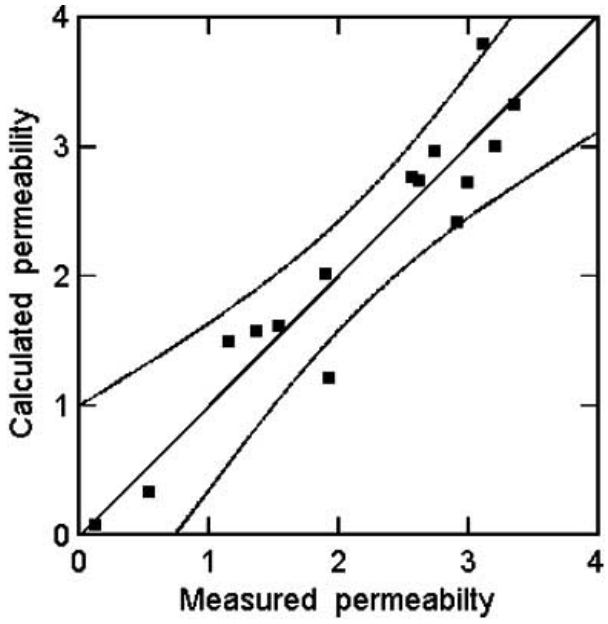

Fig. (2). Experimentally obtained permeability of Ca^{2+} in relation to that of Cs^{+} (P2X2 and mutants of P2X2 [4]), and theoretically calculated permeability using an optimized backpropagation network (Table 4). The 95% confidence interval is shown (apparent outlier: MUT05 of Table 2). Although the fitted scores do not markedly differ from those of Fig. 1, overfitting cannot be ruled out (Table 4).

Visualization of the QSAR Results by a 3D-Model of the Channel

Using the QSAR equation (3), forecasts of the permeability of mutants can be calculated. With respect to N333, T336, T339, S340, and Asp349, there is a general rank order to reduce the calcium permeability as follows: deletion of the residue without replacement may produce the largest effect, followed by W > F > L > I (the degree of the permeability changes varies in dependence on the positions).

Table 4. Weights and Current Adjustment Deltas of an Optimized Backpropagation Network. Input Layer with Two Nodes (fac-1, fac-2), Linear Transfer Function; One Hidden Layer with Two Nodes, Sigmoid Transfer Function; Output Layer with One Node (Permeability), Sigmoid Transfer Function. Training Information: Error: 0.06, Learning Rate: 0.3, Momentum Factor: 0.8. Due to the Number of Weights Compared with the Sample Size, an Overfitting Cannot be Ruled Out.

Layer	Node	Connection	Weight	Weight delta
2	1	1	-5.41924	-0.000067
2	1	2	-0.67778	0.000013
2	2	1	1.42559	0.000112
2	2	2	-0.36081	0.000104
3	1	1	6.74336	0.000126
3	1	2	-1.80875	-0.000099

The negatively charged Asp349 which lies on the internal side of the intracellular end of the gate/filter (Fig. (**3**)) is of particular interest. It is expected that replacements of Asp349 by the positively charged Arg and Lys on the one hand (predicted permeabilities: 3.0 and 3.3), by the negatively charged Glu (predicted permeability: 3.2), or by the uncharged and hydrophilic Ser and Thr (predicted permeabilities: 3.2 and 2.4) do not reduce markedly the calcium permeability.

The predictions support the hypothesis that residues which (i) put into the cavity and (ii) contribute to hydrogen bonding forces, are involved in the control of the transport of hydrated cations through the P2X channel. A replacement of these residues by nonpolar hydrophobic amino acids may destroy the binding with hydrated cations and, in addition, may sterically hinder the cationic flux. The question raised whether this hypothesis can be visualized at an atomistic level using a dimeric P2X channel construct. For exemplary purpose, the replacement of Asp349 by the nonpolar, hydrophobic, medium-sized Ile is modelled (Fig. 3). And indeed, it can be seen that the cationic flux will be hindered because Ile does not have hydrogen bonding properties. Using eq. (3), the predicted permeability is 0.27, that is, the permeability will strongly be reduced.

To avoid semantic confusion, it should be noted that "prediction" is defined in a probabilistic sense. Matches to generic rules do not mean "this is true" but rather "this might be true". Only biological and chemical knowledge can determine whether or not these predictions are meaningful. Thus, the results from the computational tools are probabilistic predictions and subject to further experimental verification. It is hoped that an experimental proof of the

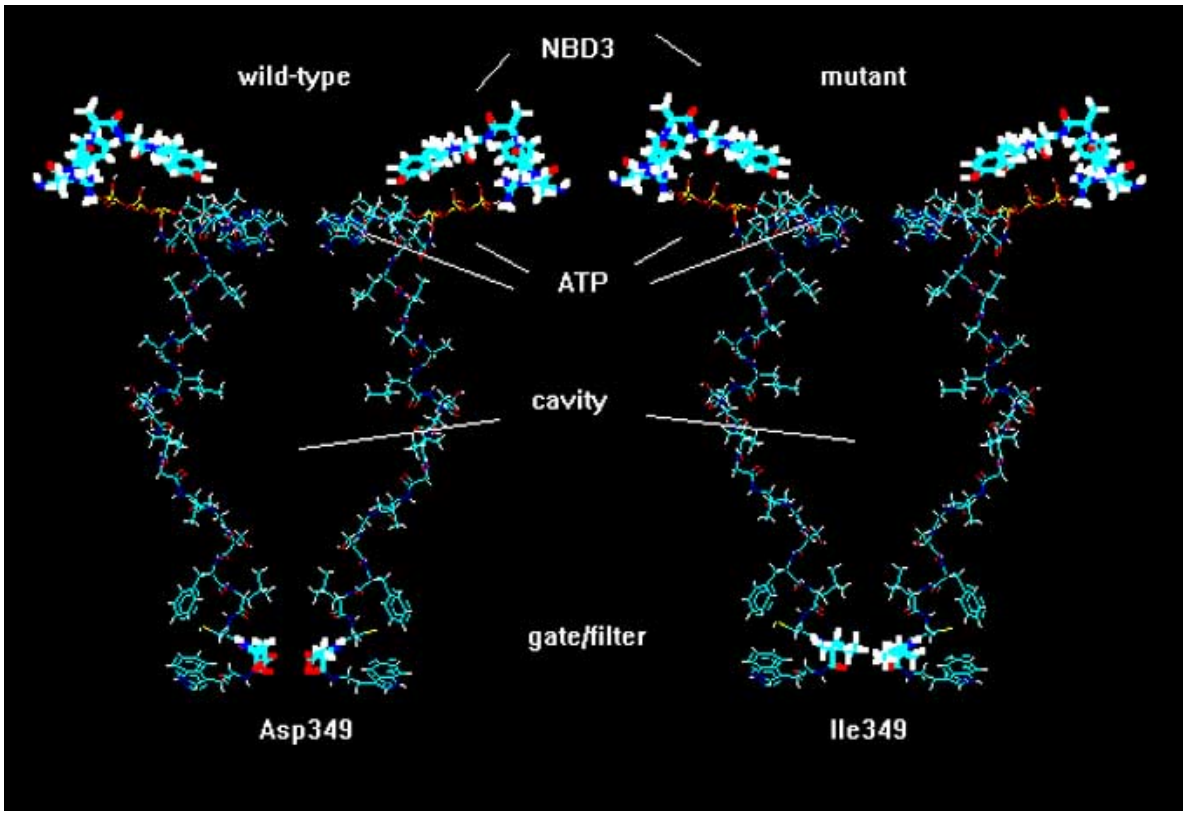

Fig. (3). Model of the open state of the negatively charged channel-forming domain of the membrane-embedded P2X2 receptor subunit (rat) of a wild-type and mutant form. Asp349 lies on the internal side of the gate/filter domain. The replacement of Asp349 (native form) by Ile349 (mutant) will produce a reduced permeability of Ca^{2+} in relation to that of Cs^{+} due to the loss of hydrogen bonding forces (measured value of the wild-type form with Asp349: 2.74, predicted value of the mutant with Ile349: 0.27). Two of the functionally 3n homomeric symmetric P2X2 subunits (n = 1,2,3) are shown. The fold of the channel is viewed perpendicular to the channel axis. The mouth of the cavity (330-341) is given at the top of the diagram, and the gate/filter region (342-350) at the bottom. The pentapeptide RFAKY (290-294) contributes to the third adenine nucleotide binding domain NBD3 of the ECD. After ATP binding, a conversion of the gate/filter occurs (open state). The conformationally flexible gate/filter segment consists of a transmembrane part (342-347) of the TMD2 and an intracellular part (348-350) of the ICD2. The following attachment sites of the P2X2 receptor subunit were predicted [2]: protein kinase C phosphorylation sites: 18-20, 116-118, 205-207, 272-274, 302-304, 363-365, 372-374, 377-379, 426-428; tyrosine protein kinase phosphorylation sites: 79-86, 274-280; casein kinase II phosphorylation sites: 54-57, 60-63, 74-77, 100-103, 112-115, 126-129, 263-266, 413-416, 457-460, 462-465; N-glycosylation addition sites: 182-185, 239-242, 298-301; glycosaminoglycan addition site: 408-411. Therefore, the Thr and Ser residues of the channel are fully available for a channel function. The gate/filter includes the subsequence 344-349 (GSFLCD) with the putative membrane-lipid attachment site Gly344. Colors: green, carbon; red, oxygen; white, hydrogen; blue, nitrogen; yellow, sulfur).

predicted activity of the Asp349Ile mutant will lead to a similar result.

PERSPECTIVES IN DRUG DESIGN

P2X receptor antagonists such as suramin, 4,4'-diisothiocyanatostilbene-2,2'-disulfonic acid (DIDS), pyridoxal phosphate-6-azophenyl-2',4'-disulfonic acid (PPADS), and 2'-3'-*O*-2,4,6-trinitrophenyl-ATP (TNP-ATP), lack high affinity and specificity for individual P2X receptor subtypes. The traditionally used antagonists may be categorized into structurally diverse classes with planar (e.g., suramin, DIDS, PPADS) and nonplanar conformation (e.g., TNP-ATP).

An example of a competitive antagonist with a planar conformation is a new suramin derivative, NF449. Is a selective antagonist of the human P2X1 receptor subunit [20]. Two novel lead structures have a nonplanar conformation, however. The Abott compound A-317491 (S-enantiomer) seems to be the first potent and selectively acting nonnucleotide antagonist of P2X3 and P2X2/P2X3 receptors [21]. It shows only a very poor or no affinity for a large number of other cell surface receptors, ion channels, and enzymes. The specificity of its competitive antagonist action is supported by the significant weaker activity of the R-enantiomer. The P2X3 receptor block is rapid in onset. The antagonist is not susceptible to metabolic dephosphorylation like TNP-ATP. It reduces chronic inflammatory and neuropathic pain in the rat and is metabolically stable *in vivo*.

Recently, it was found that derivatives of 1-*N*,*O*-bis(1,5-isoquinolinesulfonyl) - *N* - methyl - L-tyrosyl)-4-phenylpiperazine (KN-62) are very potent antagonists for the human P2X7 receptor [22,23]. The KN-62 derivatives are inhibitors of the calcium/calmodulin-dependent protein kinase type II and blocks currents in cell expressing the human P2X7 receptor subunit. Based on a high-thoughput screening in combination with a full lead optimization, an adamantine indazole amide has been developed and screened as novel lead compound of potent P2X7 antagonists [24].

The success of high-throughput docking [24,25] depends on a three-dimensional structure of a foregiven protein target and an algorithm that orients the candidate molecule in the active site of the proper binding pocket. Although experimentally based details on P2X receptor architecture (X-ray and NMR analysis) are unknown at the atomic resolution level up to now, this study has shown that QSAR and molecular modelling of the P2X2 channel may lead to the discovery of active sites. On the other hand, candidates of selectively acting P2X2 antagonists are not available in open literature [1]. A new *de novo* design, the receptor-based algorithm [26], may be useful to sequentially build up P2X2 ligands which are predicted to interact with the surface of the active channel sites. This work is under progress.

Received: 10 September, 2004 Accepted: 05 October, 2004

ACKNOWLEDGEMENT

This work was supported by the Deutsche Forschungsgemeinschaft (DFG, IV 20/11-1).

REFERENCES

[1] North, R. A. *Physiol. Rev*., **2002**, *82*, 1013.
[2] Mager, P. P.; Weber, E.; and Illes, P. *Curr. Topics Med. Chem*., **2004**, *4*, 000
[3] Thompson, J. D.; Higgins, D. G.; Gibson, T. J. *Acids Res*., **1994**, *22*, 4673.
[4] Migita, K.; Haines, W. R.; Voigt, M. M.; Egan, T. M. *J. Biol. Chem.*, **2001**, *276*, 30934.
[5] Finkelstein, A. V.; Ptitsyn, O. H.; Kozitysin, S. A. *Biopolymers*, **1977**, *16*, 497.
[6] Mager, P. P. *Med. Res. Rev*., **1997**, *17*, 235.
[7] Kyte, K.; Doolittle, R. F. *J. Mol. Biol*., **1982**, *157*, 105.
[8] Eisenberg, D.; Schwarz, E.; Komaromy, M.; Wall, R. *J. Mol. Biol*., **1984**, *189*, 125.
[9] Eroshkin, A. M.; Formin, V. I.; Zhilkin, P. A.; Ivanisenko, V. V.; Kondrakhin, I. V. *Comput. Appl. Biosci*., **1995**, *11*, 49.
[10] Mager, P. P. *Design Statistics in Pharmacochemistry*, John Wiley: New York, **1991**.
[11] Wold, H. in *Research Papers in Statistics: Festschrift for J. Neuman*; David, N. Ed.; Wiley: New York, **1966**, pp. 411-444.
[12] Butler, A. N.; Denham, M. C. *J. R. Statist. Soc. B*, **2000**, *62*, Part 3, 585.
[13] Mager, P. P. *Med. Chem. Res*., **1998**, *8*, 277.
[14] Mager, P. P.; Reinhardt, R. *Mol. Simul*., **2000**, *28*, 287.
[15] Evans, R. J.; Lewis, C.; Virginio, C.; Lundstrom, K.; Buell, G.; Surprenant, A.; North, R. A. *J. Physiol*., **1996,** *497*, 413.
[16] Virginio, C.; North, R. A., and Surprenant, A. *J. Physiol*., **1998**, *510*, 27.
[17] Hansch, C. in *Drug Design*; Ariens, E. J., Ed.; Academic Press: New York, **1971**, Vol. 1, pp. 271-342.
[18] Mager, P. P. *J. Chemometrics*, **1996**, *10*, 221.
[19] Mager, P. P. *J. Chemometrics*, **1995**, *9*, 211.
[20] Hülsmann, M.; Nickel, P.; Kassack, M.; Schmalzing, G.; Lambrecht, G.; Markwardt, F. *Eur. J. Pharmacol* **2003**, *470*, 1.
[21] McGraughty, S.; Wismer, C. T.; Zhu, C. Z.; Mikusa, J.; Honore, P.; Chu, K. L.; Lee, C.-H.; Faltynek, C. R.; Jarvis, M. F. *Br. J. Pharmacol*., **2003**, *140*, 1381.
[22] Gargett, C. E.; Wiley, J. S. *Br. J. Pharmacol*., **1997**, *120*, 1483.
[23] Baraldi, P. G.; Del Carmen Nunez, M.; Morelli, A.; Falzoni, S.; Di Virgilio, F.; Romagnoli, R. *J. Med. Chem*., **2003**, *46*, 1318.
[24] Baxter, A.; Bent, J.; Bowers, K.; Braddock, M.; Brough, S.; Fagura, M.; Lawson, M.; McInally, T.; Mortimore, M.; Robertson, M.; Weaver, R.; Webborn, P. *Bioorg. Med. Chem. Lett*., **2003**, *13*, 4047.
[25] Klon, A. E.; Glick, M.; Thoma, M.; Acklin, P.; Davies, J. W. *J. Med. Chem*., **2004**, *47*, 2743.
[26] Honma, T.; Hayashi, K.; Aoyama, T.; Hashimoto, N.; Machida, T.; Fukasawa, K.; Iwama, T.; Ikeura, C., Ikuta; M., Suzuki-Takahashi, I.; Iwasawa, Y.; Hayama, T.; Nishimura, S.; Morishima, H. *J. Med. Chem*., **2001**, *44*, 4615.